

# A Rock Catalogue Data Study for Extending NMR Fluid Substitution to Sandstone

Holger Thern\*

Baker Hughes, 29221 Celle, Germany

**Abstract.** NMR fluid substitution applied to NMR well log data is a method for estimating the  $T_2$  distribution of a porous medium fully saturated by water from a measured  $T_2$  distribution with partial water saturation. The underlying goal is to uncover pore space information that is obscured by the presence of hydrocarbon (HC) or potentially also  $\text{CO}_2$  in subsurface formations. The method employs a simple, theory-derived relationship between water saturation ( $S_w$ ) and the average, i.e., geometric mean, water peak position in the NMR  $T_2$  distribution ( $T_{2gm}$ ), and it was initially developed for water-wet chalk with a mono-modal pore size distribution. This study investigates the application of NMR fluid substitution for water-wet sandstone based on 352 core plugs with NMR data acquired at full and irreducible  $S_w$ . Key is the application of a spectral cutoff ( $T_{2cut,stat}$ ) that separates the  $T_2$  distribution of the water component into a static water fraction (corresponding to pores too small to contain non-wetting-phase fluids such as HC, air, or  $\text{CO}_2$ ) and a changeable water fraction (corresponding to pores large enough to contain non-wetting-phase fluids). The changeable water fraction is subsequently increased and shifted according to the established relationship between  $T_{2gm}$  and  $S_w$ . Very good agreement between measured and estimated  $T_2$  distributions at full water saturation is achieved for  $T_{2cut,stat}$  estimated at one third of the standard bound-water  $T_2$  cutoff ( $T_{2cut}$ ), validating the NMR fluid substitution approach for sandstone.

## 1 Introduction

### 1.1 Motivation

The NMR fluid substitution method as discussed in this study was initially developed for water-wet chalk with a mono-modal pore size distribution [1]. It was validated by rock catalogue data [2, 3] and in additional core data studies and well log data applications [4, 5]. The idea of NMR fluid substitution is to eliminate the influence of non-wetting fluids in the pore space such as hydrocarbon (HC), air, or  $\text{CO}_2$  and to estimate the  $T_2$  distribution at full water saturation. The  $T_2$  distribution at full water saturation does not suffer from interfering HC signal components or from a not existing air or  $\text{CO}_2$  signal and, therefore, reflects pore space characteristics such as pore radius and matrix permeability more accurately.

In the past 10 years, the application has attracted the attention of operators, service providers, and academia, with increasing interest in extending NMR fluid substitution to more complex rock types such as sandstone. Therefore, it must account for wider pore size distributions resulting in overlapping  $T_2$  responses from fully and partially water saturated pores. More complex pore structures such as the presence of connected and disconnected vugs, macro-porosity, fractures, or changes in wettability, which are not for instance common in carbonates, are not part of the study.

Following the successful sandstone extension of NMR fluid substitution, the automation of the application is addressed in the study, too. It enables core and well log data processing with minimum user interaction for both mono-modal chalk and sandstone formations.

### 1.2 Background

The initial idea of NMR fluid substitution links the theoretic derivation of the NMR  $T_2$  relaxation time of a fluid-filled pore with observations from NMR measurements on core. The proportionality between the  $T_2$  value (in seconds) of a fluid-filled pore and the pore radius  $r$  (in  $\mu\text{m}$ ) is one of the fundamentals of NMR relaxation time interpretation

$$\frac{1}{T_2} = \rho \cdot \frac{SA}{V} = \rho \cdot \frac{\alpha}{r} \quad (1)$$

with  $\rho$  = surface relaxivity [ $\mu\text{m/s}$ ] (material constant),  $SA$  = pore surface area [ $\mu\text{m}^2$ ],  $V$  = pore volume [ $\mu\text{m}^3$ ],  $\alpha$  = geometry factor [unitless] (1 for crack, 2 for cylinder, 3 for sphere). The relationship is valid, when bulk and diffusional  $T_2$  relaxation terms can be neglected, which is usually the case for the water phase due to surface relaxation in water-wet pore systems at small enough magnetic field gradients.

Laboratory measurements on chalk core at several water saturations show how the water  $T_2$  relaxation time continuously reduces when a non-wetting phase fluid

\* Corresponding author: [holger.thern@bakerhughes.com](mailto:holger.thern@bakerhughes.com)

such as oil is introduced into the pore space [4-7], suggesting a fluid-film model behaviour of the water phase [1]. Based on the fluid-film model behaviour, the measured  $T_2$  of the wetting-phase fluid in a single pore is a function of the saturation of the wetting-phase fluid. Therefore, the  $T_2$  of a wetting-phase fluid measured at one saturation in a pore can be converted to the  $T_2$  of the same wetting-phase fluid at another saturation. A challenge of particular interest is to estimate the  $T_2$  of water-filled pores based on well log measurements of an ensemble of water-wet pores partially filled with HC or CO<sub>2</sub>, hence the terminology NMR fluid substitution. The  $T_2$  response of water-filled pores provides a much more direct access to pore space characteristics such as pore radius and matrix permeability.

The method found very successful application for NMR well log data in North Sea chalk [4, 5]. The conducted core studies confirm that the  $T_2$  distributions measured at several water saturations behave as predicted by the fluid-film model and that a light HC can be easily identified and quantified by a simple  $T_2$  cutoff approach. The core measurements also confirm a relatively narrow, virtually mono-modal pore size distribution, which enables to represent the ensemble of pores measured by NMR by an average pore size and an average  $T_2$  (i.e., geometric mean),  $T_{2gm}$ .

Several research teams have worked on refining the film model approach for non-unimodal  $T_2$  pore size distributions [e.g., 8], finding alternative solutions [e.g., 9], and extending the approach to multi-modal carbonates [10] and sandstone [11]. On one hand, this study builds upon the initial fluid-film model idea using the same rock catalogue for developing a sandstone NMR fluid substitution algorithm that was used for the chalk NMR fluid substitution algorithm [1]. On the other hand, the study incorporates to a considerable degree results from earlier sandstone NMR fluid substitution investigations [8, 11].

The initial investigations and the study presented here are based on  $T_2$  relaxation times. The NMR fluid substitution approach applies, however, also for  $T_1$  relaxation times. A major difference between  $T_1$  and  $T_2$  measurements is the diffusion sensitivity of the  $T_2$  data. Since the diffusion effect for water under water-wet conditions for small enough magnetic field gradients can be considered negligible, the NMR fluid substitution applies in the same way to a  $T_1$  distribution as to a  $T_2$  distribution. Differences in bulk  $T_1$  versus  $T_2$  and surface relaxivity may also result in somewhat different component decomposition for  $T_1$  versus  $T_2$  distributions such as cutoff placement.

### 1.3 Rock catalogue

The ART (Applied Reservoir Technology) rock catalogue compilation [2, 3] was a joint effort of multiple industry partners to establish common grounds for understanding low-field NMR response in conventional formations (i.e., sandstone and carbonates). The program was initiated in 1994 and carried out over several years. The NMR Sandstone Rock Catalogue [2] contains 380 sandstone core samples from 19 oil and gas fields provided by 19 different operators. More than half of the sandstone core

samples originate from the North Sea, but other regions around the world (Europe, USA, Middle East) are represented as well. The complementary NMR Carbonate Rock Catalogue [3] contains 108 carbonate samples evenly divided into six types: chalk, diagenetic chalk, microcrystalline dolomite, oolitic limestone, sucrosic dolomite, and vuggy dolomite.

Most important for this study are the NMR  $T_2$  data acquired at a frequency of 2 MHz with an inter-echo spacing  $TE$  of 0.35 ms using an Oxford Instruments laboratory device. The  $T_2$  data are available for full and irreducible water saturation,  $S_w = 1$  and  $S_{wir}$ , respectively. The irreducible water saturation condition was achieved by centrifuging the core. The procedure is described only briefly [3]: “Desaturate core in gas using the automated ultracentrifuge. Set automated centrifuge to monitor production rate at 5.5 bar capillary pressure. Stop experiment when rate reaches 0.15 ml/hour. Determine  $S_{wi}$  using the normal procedure.”

Several more core measurements were conducted, and additional information was compiled for the catalogues:

- Standard core data including Helium porosity, Klinkenberg permeability, grain density, and formation resistivity factor
- BSEI (backscattered electron image) data, e.g., for pore size distribution, pore geometry, and mineral fractions
- XRD (X-ray diffraction) data, e.g., for mineralogical information such as clay type and content
- XRF (X-ray fluorescence) data, e.g., for elemental and oxide identification and quantification
- MICP (mercury injection capillary pressure) data, e.g., for pore throat size distribution, entry pressure, and closure pressure
- CT (computed tomography) images, e.g., for visual representation of the core sample and for fracture identification
- Additional information such as the age of the formation as well as the geologic and depositional environment.

Core samples with incomplete or corrupted NMR data sets were identified and excluded from the study. For applying NMR fluid substitution meaningfully, sufficient water signal needs to be present at  $S_{wir}$ . Samples with  $S_{wir}$  smaller than 0.05 were excluded, because uncertainties will get amplified by a factor larger than 20 when scaling from less than 0.05 to full water saturation. Two samples were excluded because the  $T_2$  distributions at  $S_w = 1$  and  $S_{wir}$  show very prominent inconsistent features. Two more samples were excluded, because the  $T_2$  distributions show late  $T_2$  components well above 100 ms that appear not reasonable for a sandstone with  $S_{wir}$  as low as 0.15 and 0.22, respectively. It is suspected that problems occurred during the preparation of these four samples.

From visual inspection, several more of the remaining 352  $T_2$  distributions appear disputable. Since the visual identification of unexpected  $T_2$  distribution features and inconsistencies between  $S_w = 1$  and  $S_{wir}$  data is rather subjective, no further reduction of the data set was applied, keeping also the less convincing data sets.

During the initial evaluation of the rock catalogue data, the chalk data were used to validate the film model and to develop the NMR fluid substitution method for simple, mono-modal pore systems that are common for a considerable number of chalk reservoirs. The sandstone data, however, showed a considerable, albeit systematic, deviation from the chalk film model behaviour. At the time it was reasoned that the observed sandstone behaviour can be explained by two sets of pores. A first set of pores behaves according to the film model, while a second set of pores is static, i.e., the pores keep their  $T_2$  position independent of the overall saturation condition. In other words, the first set of pores contains both bound water and HC, while the second set of pores contains only bound water [1]. The behaviour was meanwhile confirmed as documented by the successful NMR fluid substitution for two Berea sandstone core samples [11].

## 2 Theory

### 2.1 TSR Relationship

Based on equation (1), the  $T_{2gm}$  of a partially water-filled pore is proportional to its volume-to-surface ratio if water is the wetting-phase fluid. If the volume (i.e., saturation) of water changes, the surface area remains the same and, thus,  $T_{2gm}$  is proportional to  $S_w$ . For two different  $S_w$  conditions, e.g.,  $S_{wir}$  and  $S_w = 1$ , the  $T_{2gm}$  of an ensemble of water-wet, well-connected pores of similar pore size is given by the  $T_2$ -saturation-ratio (TSR) relationship [1]

$$\frac{T_{2gm}(S_{wir})}{T_{2gm}(S_w=1)} = \frac{S_{wir}}{1} \quad (2).$$

**Fig. 1** compiles the TSR behaviour for the rock catalogue data divided into three groups. The mono-modal chalk and diagenetic chalk samples (top) follow the TSR film model very well. The sandstone samples (middle) come with a wide variety of properties (such as mineralogy, grain sorting, and clay content) and show a considerable, albeit systematic, deviation from the TSR film model behaviour. The correlation to various rock properties was inspected but there is no simple link between the deviation to a single property. It appears, however, that grain sorting and clay content play a more prominent role, since the clean and well-sorted samples follow a similar trend in the TSR plot. This raises the concern that an NMR fluid substitution for sandstone could be limited to clean and well-sorted formations. The more complex carbonate samples (bottom) show a much more erratic deviation than the sandstone samples. The correlation between TSR film model deviation and carbonate rock properties (such as pore connectivity, fractures, etc.) remains yet to be explored in detail. The data suggest, however, that a simple universal NMR fluid substitution for complex carbonates may not be feasible.

### 2.2 Component Separation

The separation of different fluid components in the  $T_2$  distribution is a prerequisite for the successful application

of NMR fluid substitution. The fluid components include HC, clay-bound water (CBW) or micro-porosity, as well as water, covering both bound and movable fractions. If applicable, the component separation is most straightforward by appropriate cutoffs in the  $T_2$  distribution.

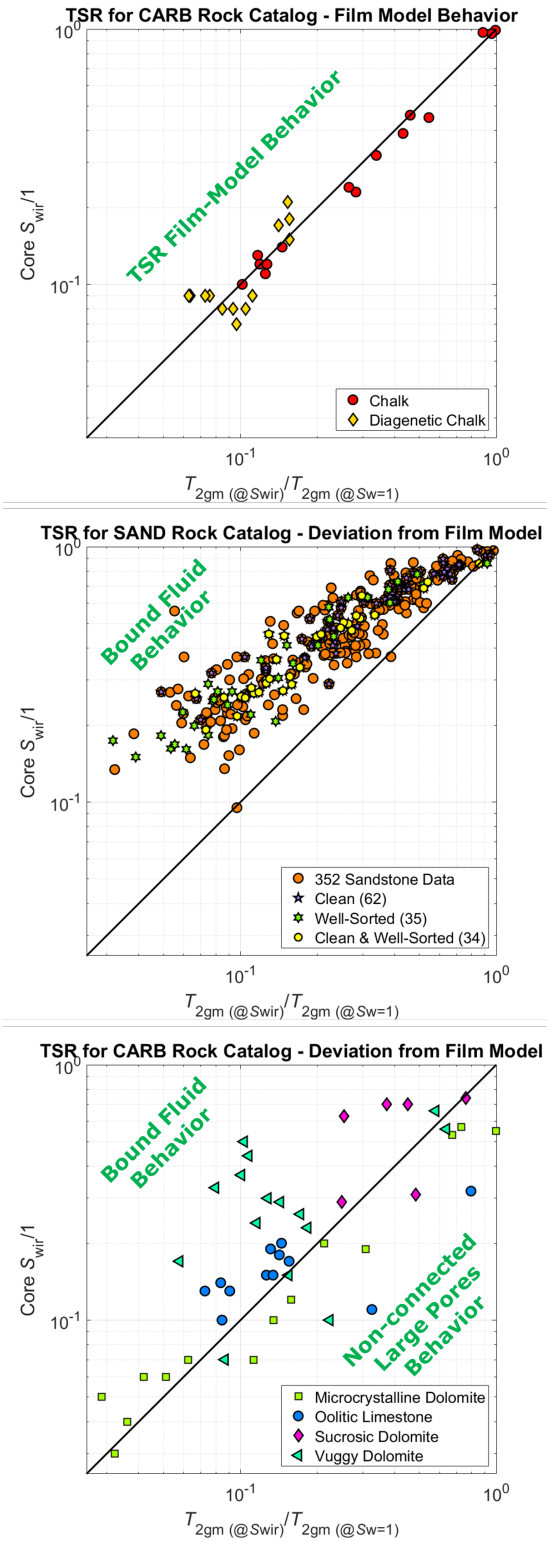


**Fig. 1.**  $T_2$ -saturation-ratio (TSR) relationship for three rock types: Mono-modal chalk (top), widely varying sandstone (middle), more complex carbonates (bottom). The chalk data behave as predicted by the fluid-film model. The sandstone data show an overall systematic deviation. The more complex carbonates show rather erratic deviations.

A light HC for instance occurs at long  $T_2$  values, which are usually not reached by the water phase due to surface relaxation in water-wet pores. CBW and micro-porosity are typically separated from other water components at very short  $T_2$  values. Other approaches for fluid component separation may involve 2D-NMR to identify HC based on its diffusivity or the fitting of multiple peaks (e.g., Gauss or Gamma functions) to the NMR data, with each peak representing a different fluid component. For the rock catalogue data, no HC peak identification and quantification is necessary, because only water and air are in the pore space at  $S_{wir}$  and the saturation of the non-wetting air is accordingly given by  $1 - S_{wir}$ .

In sandstone formations with multiple pore sizes or a relatively wide pore size distribution, pores with different saturations (i.e., small pores with  $S_w = 1$  and larger pores with  $S_w < 1$ ) can have the same  $T_2$  [8]. An elegant method for separating the two overlapping sets of pores is a spectral  $T_2$  cutoff [11, 12]. The spectral  $T_2$  cutoff assigns a fraction of the water  $T_2$  peak to a *static* component (representing relatively small pores at  $S_w = 1$ ) and the other fraction of the water  $T_2$  peak to a *changeable* component (representing relatively large pores at  $S_w < 1$ ).

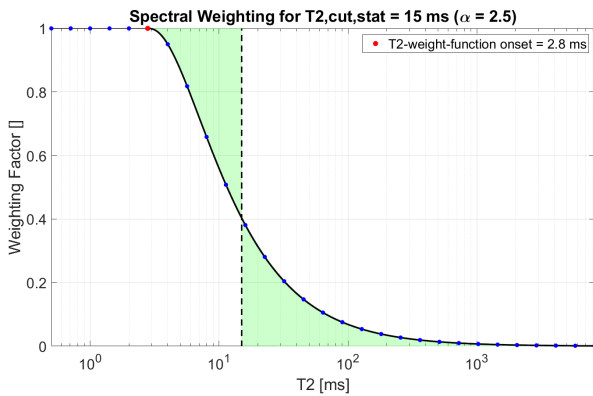


**Fig. 2.** Weighting function for a spectral  $T_2$  cutoff at 15 ms for a geometry factor  $\alpha = 2.5$ .

**Fig. 2** shows the weighting function for a spectral  $T_2$  cutoff at 15 ms for a geometry factor  $\alpha = 2.5$ . The latter represents a fifty-fifty mixture of cylindrical and spherical pores, which is considered a reasonable assumption for a typical sandstone pore network. **Fig. 3** shows a well log data example from a shaly sand at  $S_w < 1$ . Three fluid components, CBW/micro-porosity (i.e., early  $T_2$  peak), light HC (i.e., late  $T_2$  peak), and a water  $T_2$  peak can be identified visually and separated by standard peak separation methods such as a step-function  $T_2$  cutoff. The spectral  $T_2$  cutoff at 15 ms is applied for separating the water  $T_2$  component into static and changeable fractions.

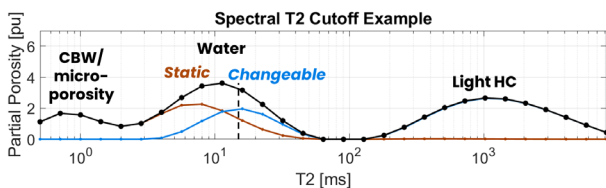


**Fig. 3.** Spectral  $T_2$  cutoff application separating the water  $T_2$  peak into a static (red) and a changeable (blue) fraction for  $T_{2cut,stat} = 15$  ms.

While the  $T_2$  cutoffs for CBW/micro-porosity vs. water vs. HC can be identified visually, the position of the spectral  $T_2$  cutoff between the static and the changeable water fraction,  $T_{2cut,stat}$ , has yet to be determined. It will be estimated when discussing the application of the NMR fluid substitution method to the core data in chapter 3. It can, however, already be reasoned that  $T_{2cut,stat}$  is smaller than  $T_{2cut}$  because the bound water fraction from  $T_2$  cutoff application for a HC-bearing sandstone at  $S_{wir}$  contains not only static but also changeable water fractions.

Only the changeable fluid fraction is attributed to water residing in pores at  $S_w < 1$ . Therefore, only this component will be used for applying the TSR relationship given in equation (2) when performing the NMR fluid substitution. The other two water components, i.e., CBW/micro-porosity and the static water component, remain unaltered and can be handled as one component.

## 2.3 Optional Widening

Application of the spectral  $T_2$  cutoff yields a changeable water response that covers a considerable range in the  $T_2$  distribution. For a substantial number of rock catalogue samples, the changeable water  $T_2$  peak after NMR fluid substitution appears to be slightly too narrow. Speculations about the reason include the following physical and mathematical effects:

- Under certain circumstances (e.g., very small water saturation, resulting in a very narrow water  $T_2$  peak), the changeable  $T_2$  distribution fraction can become too narrow, possibly not reflecting the complete extent of the pore size distribution.
- The interaction between adjacent pores is different for partially water-filled pores (in particular if the saturation is very small) compared to the fully water-saturated pores. A known effect is the diffusive coupling which may look like a smearing effect across two or more  $T_2$  distribution peaks.
- The peak width in  $T_2$  distributions is driven by a complex interaction between signal-to-noise ratio (SNR) and the selected regularization (e.g., curvature smoothing) that is applied during the inversion of the echo train data to the  $T_2$  distribution.

For compensating an apparently too narrow changeable  $T_2$  distribution, the implemented NMR fluid substitution method offers an optional peak widening. The amount of widening is limited to not extend beyond the onset of the spectral weighting function (see Fig. 2). It is also scaled proportional to the amount of fluid to be substituted (i.e.,  $1/(1 - S_w)$ ), so that for example no widening occurs if  $S_w$  is close to 1.

## 3 Application

### 3.1 Workflow

Having defined the prerequisites and processing steps, the NMR fluid substitution can be applied to the sandstone rock catalogue data in the following 6 steps:

1. Compile  $T_2$  distributions measured at both  $S_w = 1$  and  $S_{wir}$  for the 352 valid core samples.
2. Apply the spectral cutoff  $T_{2cut,stat}$  to separate static and changeable water fractions. Where applicable, the static water fraction includes CBW/micro-porosity, which remains unaltered.
3. Determine the saturation of the changeable water fraction  $S_{w,ch}$  in relation to the porosity without the static water fraction. The corresponding non-wetting phase fluid saturation (which is air for the rock catalogue samples) corresponds to  $1 - S_{w,ch}$ .
4. Apply NMR fluid substitution to the changeable water fraction according to equation (2), i.e., shift the  $T_2$  distribution and increase its signal strength by  $1/S_{w,ch}$ .
5. Optionally, widen the resulting  $T_2$  distribution.
6. Combine the resulting  $T_2$  distribution with the earlier separated static water fraction for the final result.

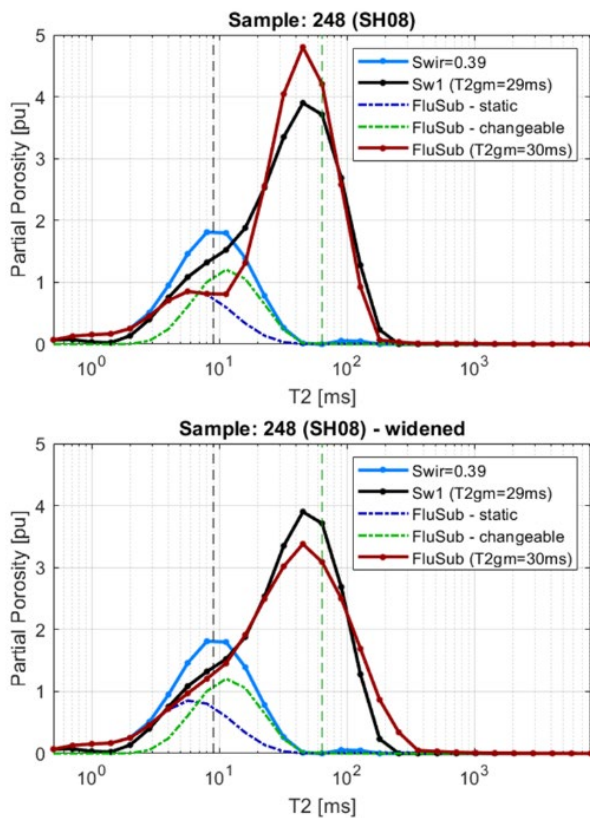


**Fig. 4.** Application of the NMR fluid substitution to the core sample number 248 without widening (top) and with widening (bottom). Several  $T_2$  distributions are shown: measured at  $S_{wir}$  (light blue); measured at  $S_w = 1$  (black); static fraction at  $S_{wir}$  (dash-dot dark blue); changeable fraction at  $S_{wir}$  (dash-dot green); and from NMR fluid substitution (dark red).

**Fig. 4** illustrates the workflow by showing data from sample number 248 without widening (top) and with widening (bottom). The measured  $T_2$  at  $S_{wir} = 0.39$  is shown in light blue and the measured  $T_2$  for  $S_w = 1$  is shown in black with an estimated  $T_{2gm}$  of 29 ms. The water  $T_2$  at  $S_{wir}$  is separated into the static fraction in dash-dot dark blue (including potential CBW) and the changeable fraction in dash-dot green for  $T_{2cut,stat}$  equal to one third of the bound-water  $T_2$  cutoff value. The resulting  $T_2$  distribution after shifting and scaling the changeable fluid

fraction is shown in dark red with an estimated  $T_{2gm}$  of 30 ms for both cases with and without widening.

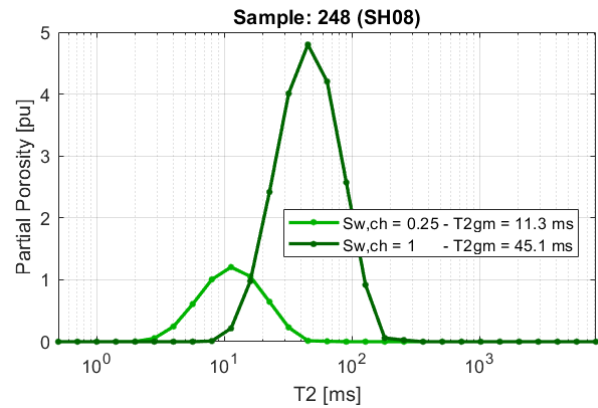


**Fig. 5.** Illustration of step 4: NMR fluid substitution scaling of the changeable water fraction (green) from  $S_{w,ch} = 0.25$  to 1 (dark green) excluding the static water fraction. Both  $T_{2gm}$  and the changeable water porosity (area under the  $T_2$  distribution) are increased by a factor 4.0. No widening is applied.

The fundamental processing step of the NMR fluid substitution is illustrated for sample number 248 in **Fig. 5**. Starting point is the changeable water fraction (green in Fig. 5, green dash-dot in Fig. 4). The static water  $T_2$  distribution (blue dash-dot in Fig. 4) remains unaltered and is excluded from the following processing steps. The position of the changeable water  $T_2$  distribution can be represented by its  $T_{2gm}$  value, and the shape is given by the  $T_2$  distribution. The saturation of the changeable water fraction without the static water fraction is  $S_{w,ch} = 0.25$  (see **Table 1**). When applying the NMR fluid substitution, the  $T_{2gm}$  of the changeable water  $T_2$  peak is shifted by  $1/S_{w,ch} = 4.0$ . The shift increases  $T_{2gm}$  of the changeable  $T_2$  distribution from 11.3 to 45.1 ms. At the same time, the NMR signal is increased by the same factor 4.0 by upscaling the bin amplitudes of the shifted  $T_2$  distribution. Note that, in this example, widening has not been applied.

**Table 1.** Fluid components for rock catalogue sample 248. The saturation of the changeable water fraction related to the porosity without the static fraction ( $S_{w,ch} = 0.25$ , row 5) is the basis for the scaling factor for the NMR fluid substitution.

Component	Porosity	Total porosity saturation	Saturation w/o static fraction
Total porosity	25 pu	1	—
Static water (incl. CBW)	4.8 pu	0.19	—
Porosity without static water	20.2 pu	0.81	1
Changeable water	5.1 pu	0.2	0.25
Static + changeable water	9.8 pu	0.39	—
Air (= non-wetting fluid)	15.1 pu	0.61	0.75

The good match of the  $T_{2gm}$  values as well as the  $T_2$  distributions measured at  $S_w = 1$  vs. the  $T_2$  distribution after NMR fluid substitution in **Fig. 4** validate the



proposed NMR fluid substitution method. The optional widening can be considered a cosmetic factor that is debatable for numerous core samples. It may, however, become more relevant for NMR well log data processing because the lower SNR may have more influence on the width of  $T_2$  peaks.

### 3.2 Comparison of $T_{2gm}$

NMR fluid substitution was applied to all 352 core samples. Fig. 6 shows the cross-plot of all measured  $T_{2gm}$  at  $S_w = 1$  (horizontal axis) vs. all  $T_{2gm}$  after NMR fluid substitution (vertical axis) using  $T_{2cut,stat}$  equal to one third of the sample-specific bound-water  $T_2$  cutoff value. An excellent correlation is observed validating the NMR fluid substitution approach. The quality of the cross-plot does not change noticeably if the conversion factor is varied between 2.5 and 3.5 indicating that the relationship between  $T_{2cut,stat}$  and  $T_{2cut}$  is critical for the method but does not require an overly sensitive adjustment.

The insert in Fig. 6 shows the NMR fluid substitution results for the same data and processing but without the widening of the changeable  $T_2$  distribution. It illustrates that a moderate widening (with the same amount as for the example in Fig. 4) has no substantial effect on  $T_{2gm}$ , which means that key petrophysical deliverables from NMR fluid substitution such as average pore size and matrix permeability are virtually not affected.

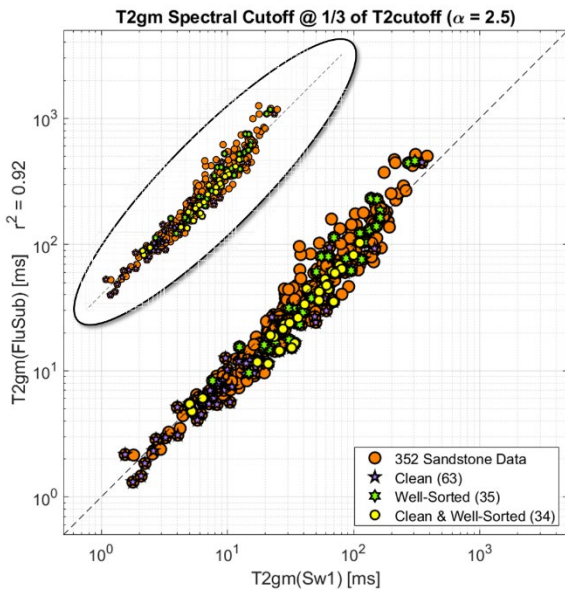


**Fig. 6.** Cross-plot of all measured  $T_{2gm}$  at  $S_w = 1$  (horizontal axis) vs. all  $T_{2gm}$  after NMR fluid substitution (vertical axis) for sandstone using a  $T_{2cut,stat}$  value estimated as  $T_{2cut}$  divided by 3. The main figure includes widening of the changeable fluid fraction, the insert shows virtually identical results without widening. An excellent correlation is observed validating the NMR fluid substitution approach.

The most impressive result of the study is that the data point spreading in Fig. 1, middle, is reduced dramatically when compared to Fig. 6. The figures include all sandstone samples independent of their mineralogic composition, clay content/distribution, grain sorting, etc.

This implies that a fundamental behaviour of sandstone formations is analytically captured and compensated for in the NMR fluid substitution method.  $T_{2cut,stat}$  and the separation of static and changeable water fractions may not be as important as the traditional  $T_2$  cutoff for quantifying bound vs. movable fluids in sandstone  $T_2$  distributions, but it may be relevant for future investigations related to more sophisticated sandstone pore space characterizations.

For standard well log applications, it is desirable to establish a numerical value for sandstone  $T_{2cut,stat}$  rather than having to estimate it from another value. A  $T_{2cut}$  value of 33 ms is commonly used for sandstone formations in the industry. The rock catalogue data evaluation yields  $T_{2cut}$  values of 10 and 110 ms for the P5 and P95 probability percentiles, respectively. The mean  $T_{2cut}$  is at 35 ms and the median  $T_{2cut}$  at 43 ms. For a conversion factor between 2.5 and 3.5,  $T_{2cut,stat}$  is accordingly expected between 10 and 20 ms, suggesting a default value of  $T_{2cut,stat} = 15$  ms. Future NMR well log data applications may indicate further fine-tuning of  $T_{2cut,stat}$ , because laboratory-derived NMR properties can change under downhole conditions.

### 3.3 Comparison of $T_2$ distributions

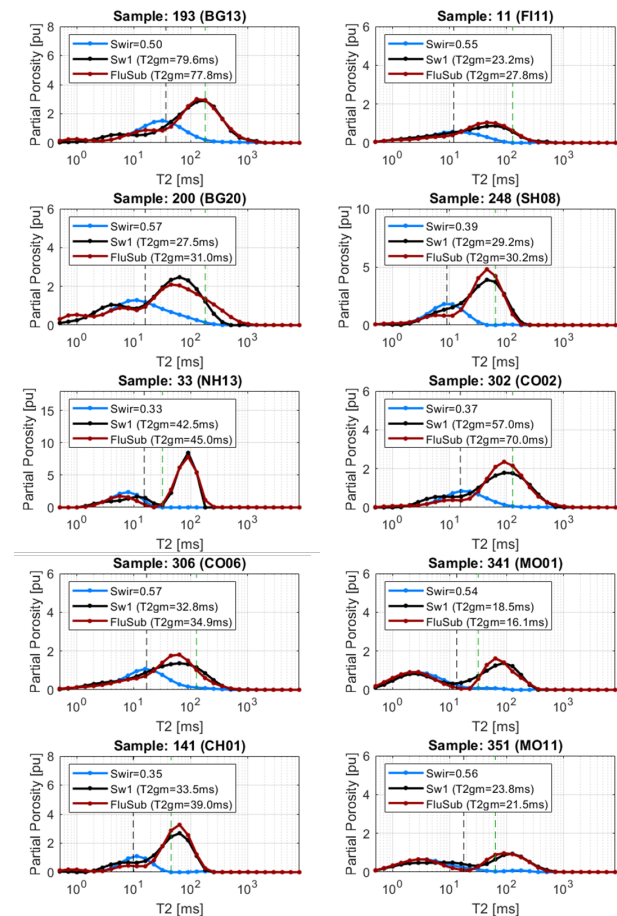


**Fig. 7.** The ten sandstone samples with the highest similarity between measured  $T_2$  distribution at  $S_w = 1$  (black) and  $T_2$  distribution after NMR fluid substitution (dark red) of the measured  $T_2$  distribution at  $S_{wir}$  (light blue). Note that the samples come from 7 different oil and gas fields / operators.

**Fig. 7** shows the  $T_2$  distributions of the ten sandstone samples with the highest similarity between the measured  $T_2$  distribution at  $S_w = 1$  (black) and the  $T_2$  distribution after NMR fluid substitution (dark red) of the measured  $T_2$  distribution at  $S_{wir}$  (light blue). Widening is included and  $T_{2cut,stat}$  is estimated as on third of  $T_{2cut}$ .

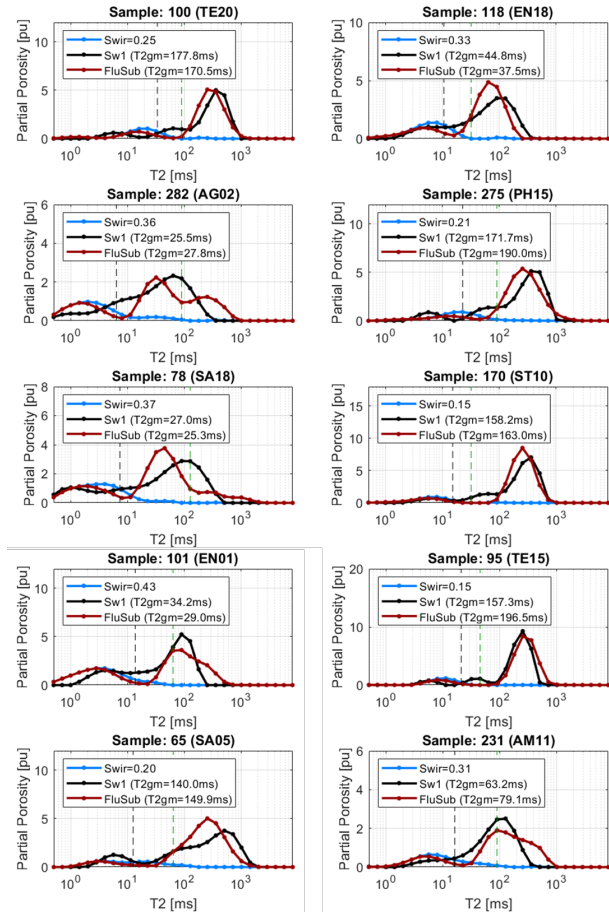


**Fig. 8.** Ten sandstone samples with average similarity between measured  $T_2$  distribution at  $S_w = 1$  (black) and  $T_2$  distribution after NMR fluid substitution (dark red) of the measured  $T_2$  distribution at  $S_{wir}$  (light blue). Note that the samples also come from 7 different oil and gas fields / operators.

**Fig. 8** shows ten sandstone samples with an average similarity between the measured  $T_2$  distribution at  $S_w = 1$  (black) and the  $T_2$  distribution after NMR fluid substitution (dark red) of the measured  $T_2$  distribution at  $S_{wir}$  (light blue). Both figures illustrate that the reconstruction of the  $T_2$  distribution at  $S_w = 1$  from a  $T_2$  distribution at  $S_{wir}$  may not always be perfect but that in general a very good to moderately good match is achieved.

The measured  $T_2$  distribution at  $S_w = 1$  and the  $T_2$  distribution after NMR fluid substitution of the  $S_{wir}$   $T_2$  distribution should be identical under ideal conditions and for perfect data. In practice, we observe an excellent match of  $T_{2gm}$  and a very good to moderately good match of the  $T_2$  distributions. In addition to the physical and mathematical reasons discussed earlier, also imperfect core data preparation and measurement conditions can be responsible for discrepancies. 30 years after the compilation of the rock catalogue, the options for quality

control (QC) are very limited. Considering potential imponderabilities and uncertainties, the NMR fluid substitution appears to work very well for the very wide variety of sandstone samples represented by the NMR Sandstone Rock Catalogue.

The approach is based on the division of the water phase into two components (static and changeable). If this does not sufficiently well capture the pore space characteristics, additional water components may be necessary. Based on the results in this study, however, no need for an additional water component was identified. This could be different when pore-space features like micro-meso-macro porosity, vugs, etc are present, as for instance expected for more complex carbonates.

The rock catalogue provides data at  $S_w = 1$  and  $S_{wir}$  conditions. The NMR fluid substitution method is, however, not limited to  $S_{wir}$  conditions, but it is expected to work at any  $S_w$  condition. Main justification comes from the earlier chalk results [4-7], where measurements were conducted at different  $S_w$  conditions. A more indirect argument is the wide range of sandstone samples in this study. It would be an extraordinary coincidence, if the method would only be valid for the specific desaturation condition available in the rock catalogue. Future log applications with varying  $S_w$  in the same lithology will provide further validation of the general applicability.

### 3.4 Automation

If an experienced user applies proven workflows to core or well log data, one can expect to get good processing results as well as an educated quality assessment for both input data and results. Depending on the complexity of data and workflows, it can, however, become a considerable challenge to automate the processing and QC, e.g., for autonomous application in a real-time system.

The NMR fluid substitution processing is currently implemented using analytical calculations in a well-defined workflow. No artificial intelligence (AI) or machine learning (ML) methods are included. The advantage of the analytical approach is that every result can be tracked from start to end and that, if needed, the algorithm can be refined and updated in a predictable manner. The development of the workflow and processing steps underwent several iterations before stable and satisfactory processing results were achieved, not only for the rock catalogue data but also for a variety of anticipated scenarios for field data.

Most parameters are pre-defined as defaults, namely the  $T_{2cut,stat}$  value, the geometry factor  $\alpha$ , the widening factor, and two  $T_2$  threshold values for fluid component identification. **Fig. 9** illustrates the default  $T_{2cut,stat}$  at 15 ms and the  $T_2$  peak identification of fluid components using default  $T_2$  thresholds at 10 and 200 ms.

In reference to the  $T_2$  thresholds at 10 and 200 ms, the  $T_2$  peak positions of two or three fluid components (i.e., CBW/micro-porosity, water, and light HC) can be identified. One or multiple  $T_2$  peaks below the lower  $T_2$  threshold of 10 ms are assigned to CBW and/or micro-porosity. One or multiple  $T_2$  peaks above the upper  $T_2$

threshold of 200 ms are assigned to light HC. The remaining peak(s) between the two thresholds are assigned to water. The fluid components are then separated and quantified by placing  $T_2$  cutoffs in the troughs between the appropriate component peaks. For sandstone, the additional spectral  $T_2$  cutoff,  $T_{2cut,stat}$  is applied for separating static and changeable water fractions.

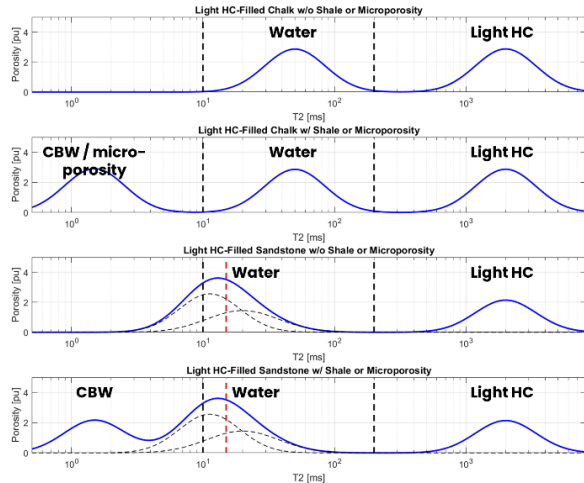


**Fig. 9.** Sketches of optimal conditions for applying NMR fluid substitution to chalk (top two) and sandstone (bottom two). Subplots 1 and 3 correspond to clean formations, subplots 2 and 4 include micro-porosity and/or CBW.  $T_2$  thresholds at 10 and 200 ms (black dashed) are used for  $T_2$  peak identification of fluid components.  $T_{2cut,stat}$  at 15 ms (red dashed) is used for separating static and changeable water fractions in sandstone.

Three items appear not suitable for automatic handling and, therefore, user interaction and input are required. The first item is to determine whether the formation is (mostly) water-wet, which is a prerequisite for the application of NMR fluid substitution. The second item is to determine the non-wetting-phase fluid that is present in the pore space. In case of light HC, the porosity and saturation can be estimated with the  $T_2$  cutoff approach as outlined above. In case of HC gas, a HI correction needs to be incorporated. In case of medium or heavy oil, the  $T_2$  cutoff method is not appropriate and other fluid component separations need to be considered. In case of liquid or gases that do not generate a proton NMR signal (e.g., air or  $\text{CO}_2$ ), the non-wetting fluid saturation needs to come from an independent source such as measurements at  $S_w = 1$  and  $S_{wir}$  like it is available in the rock catalogue. The third item is to identify the rock type, i.e., sandstone vs. chalk vs. more complex carbonates. AI and ML may be able to provide automatic rock typing and some of the non-wetting-phase fluid typing but exploring this is beyond the scope of this study.

It is not uncommon to encounter  $T_2$  distributions, which do not have one (or multiple) peaks in each of the above defined fluid component intervals (see Fig. 10). In this situation, the software checks whether a  $T_2$  distribution tail extends into the regions without peak or not. If such a  $T_2$  distribution tail exists, an appropriate  $T_2$  cutoff that is near to the  $T_2$  threshold but spaced sufficiently apart from nearby  $T_2$  peaks is estimated for component quantification.

The bottom example in Fig. 10 illustrates such a case where the upper  $T_2$  threshold appears too close to the water  $T_2$  peak. When the threshold is used as  $T_2$  cutoff, it likely overestimates the HC volume and underestimates the water volume. A solution is to shift the  $T_2$  cutoff to the  $T_2$  threshold multiplied by a defined value, e.g., 5 or 10. This is meant to reflect the condition of a major water  $T_2$  component (large and wide  $T_2$  peak) but only a minor HC component (small tail). To avoid pushing the  $T_2$  cutoff too far, the value is limited to not exceed the last  $T_2$  bin position divided by a defined value, e.g., 2 or 3. Similar considerations apply for the automated processing of some of the other cases illustrated in Fig. 10. These are attempts to translate the anticipated decisions of an experienced NMR user into meaningful and easily applicable algorithms.

Not all the considerations and features are described here in detail, because there is considerable—in part subjective—judgement involved and future results from log data applications may indicate the adjustment or fine-tuning of some of the features.

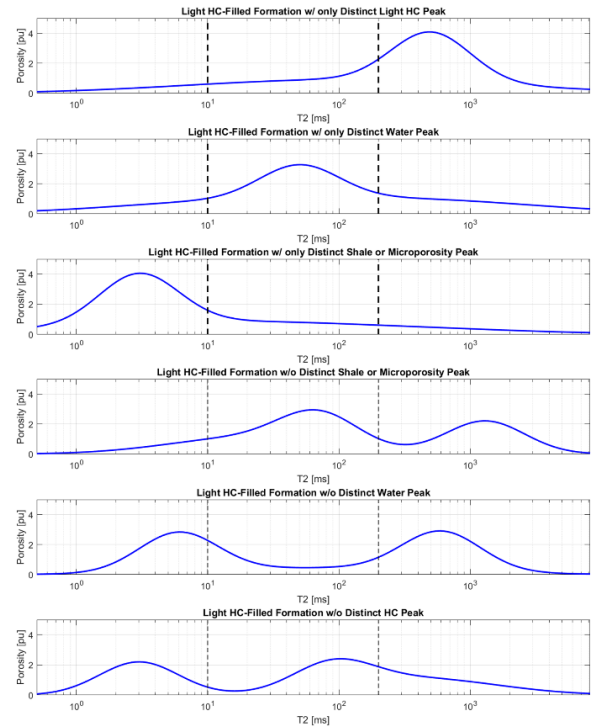


**Fig. 10.** Sketches of challenging conditions for automated application of NMR fluid substitution with either one  $T_2$  peak (top three subplots) or two  $T_2$  peaks (lower three subplots). Not all critical fluid components (CBW/microporosity, water, and light HC) can be identified and quantified by a separate peak in reference to the  $T_2$  thresholds (black dashed).

After automatic identification and quantification of the fluid components, the NMR fluid substitution is applied as described earlier. An automated quality control (QC) is introduced, which checks for instance for the identification of a distinct water  $T_2$  peak between the two  $T_2$  thresholds, since the accurate identification and quantification of the water  $T_2$  fraction is critical for the successful application of the NMR fluid substitution method.



## 4 Outlook

In the next step, the NMR fluid substitution method will be applied to NMR well log data from both chalk and sandstone reservoirs. Several memory data sets have been identified and the results will be presented in a future publication. Initial observations indicate that the method works as anticipated.

For petrophysical interpretation, the  $T_{2gm}$  from NMR fluid substitution will be converted into average pore size and matrix permeability. Essential for accurate results will be local calibrations that link NMR data to for instance MICP pore throat size distribution and core permeability in a given geologic environment.

A challenging task will be to extend the workflow to more complex carbonates. Most likely this requires more sophisticated models and additional parameters to cope with added pore space complexity such as micro-meso-macro pore systems, connected and disconnected vugs, fractures, etc. Deviations from water-wet condition due to natural processes or due to oil-based mud filtrate invasion are posing yet another difficulty to be explored.

## 5 Summary

The NMR fluid substitution method based on the fluid-film model for water-wet formations was successfully extended to sandstone formations. In contrast to simple chalk with virtually mono-modal pore size distribution, the key feature in sandstone is the usage of a spectral  $T_2$  cutoff function for separating static from changeable water fraction.

Results from 352 rock catalogue core samples illustrate the validity of the method for sandstone. Introducing static and changeable water fractions captures the pore-space characteristics of sandstones very well, independent of the geologic environment, mineralogic composition, clay content, grain sorting, etc. Particularly, the  $T_{2gm}$  values from NMR fluid substitution show an excellent correlation to the  $T_{2gm}$  values from a measurement at  $S_w = 1$ . In addition, the direct comparison of  $T_2$  distributions shows a very good to moderately good degree of similarity. The  $T_{2cut,star}$  for separating static from changeable was estimated at a default of approximately 15 ms and an optional widening of the changeable  $T_2$  distribution fraction was introduced. Further validation and potential fine-tuning will happen when the method is applied to NMR well log data.

An automated version of the processing workflow with minimal user interaction was implemented and is ready for NMR well log data processing. It includes the estimation of pore size and matrix permeability as the main petrophysical deliverables after applying NMR fluid substitution to well log data.

The comprehensive core study successfully extends the concept of NMR fluid substitution to a global application in sandstone formations. It ultimately enables more direct and accurate access to pore space information such as pore size and matrix permeability from NMR well log data in worldwide HC-bearing sandstone reservoirs.

## References

1. Them, H.: "Examining the Fluid Film Model in Porous Media by NMR Rock Catalogue Data." Paper SCA2014-51 presented at the International Symposium of the Society of Core Analysts, Avignon, France, September 8-11, 2014
2. Applied Reservoir Technology, Ltd., 1996: "The NMR Sandstone Rock Catalogue." Long Melford, U.K., Sintef Unimed
3. Applied Reservoir Technology, Ltd., 1998: "The NMR Carbonate Rock Catalogue." Long Melford, U.K., Sintef Unimed
4. Christensen, S.A., Them, H., Vejbaek, O., 2015: "NMR Fluid Substitution Method for Reservoir Characterization and Drilling Optimization in Low-Porosity Chalk." Paper HH presented at the SPWLA 56<sup>th</sup> Annual Logging Symposium, Long Beach, California, USA, July 18-22, 2015
5. Christensen, S., Them, H., Petersen, J.T., Eiane, T., 2023: "NMR Fluid Substitution – Pursuing the Fundamental Controlling Parameters of a Low Mobility Reservoir." Paper 52 presented at the SPWLA 64<sup>th</sup> Annual Logging Symposium, Lake Conroe, Tx, USA, June 10-14, 2023
6. Howard, J.J., Spinler, E.A. 1995: "Nuclear Magnetic Resonance Measurements of Wettability and Fluid Saturations in Chalk." Paper SPE 26471, Advanced Technology Series, v. 3, no. 1, p. 60-65
7. Reppert, M.G., Akkurt, R., Howard, J.J., Bonnie, R.J.M., 2005: "Porosity And Water Saturation From LWD NMR in a North Sea Chalk Formation." Paper prepared for presentation at the 46<sup>th</sup> SPWLA Annual Logging Symposium, June 26-29, New Orleans, Louisiana, United States, 2005
8. Medellin, D., Ravi, V.R., Torres-Verdin, C., 2019: "Pore-Size-Dependent Fluid Substitution Method for Magnetic Resonance Measurements." Geophysics, Vol. 84, no. 1, p. D25-D38, doi:10.1190/geo2017-0457.1
9. Minh, C.C., Jain, V., Griffiths, R., Maggs, D., 2016: "NMR T2 Fluids Substitution." Paper presented at the SPWLA 57<sup>th</sup> Annual Logging Symposium, Reykjavik, Iceland, June 25-29, 2016
10. Shao, W., Singer, G., Hursan, G., Ma, S.M., 2023: "NMR Fluid Substitution for Multimodal Carbonate Rocks." Paper 101 presented at the SPWLA 64<sup>th</sup> Annual Logging Symposium, Lake Conroe, Tx, USA, June 10-14, 2023
11. Li, B., Kesserwan, H., Jin, G., Ma, S.M., 2021: "NMR Fluid Substitution—A New Method of Reconstructing T2 Distributions Under Primary Drainage and Imbibition Conditions." Petrophysics, v. 62(4), pp. 362-378
12. Chen, S., Arro, R., Minetto, C., Georgi, D., Liu, C., 1998: "Methods for Computing SWI and BVI From NMR Logs." Paper HH presented at the SPWLA 39<sup>th</sup> Annual Logging Symposium, Keystone, Colorado, USA, 26-28 May